ELSEVIER

Biochimica et Biophysica Acta 1410 (1999) 237–247

BIOCHIMICA ET BIOPHYSICA ACTA
BBA

Aromatic amino acids in the Rieske iron–sulfur protein do not form an obligatory conduit for electron transfer from the iron–sulfur cluster to the heme of cytochrome c_1 in the cytochrome bc_1 complex

Christopher H. Snyder, Elke Denke, Bernard L. Trumpower *

Department of Biochemistry, Dartmouth Medical School, 7200 Vail, Hanover, NH 03755, USA

Received 16 December 1998; accepted 22 December 1998

Abstract

We have changed nine conserved aromatic amino acids by site-directed mutagenesis of the cloned iron–sulfur protein gene to determine if any of these residues form an obligatory conduit for electron transfer within the iron–sulfur protein of the yeast cytochrome bc_1 complex. The residues include W111, F117, W152, F173, W176, F177, H184, Y205 and F207. Greater than 70% of the catalytic activity was retained for all of the mutated iron–sulfur proteins, except for those containing a W152L and a W176L–F177L double mutation, for which the activity was $\sim$45%. The crystal structures of the bc_1 complex indicate that F177 and H184 are at the surface of the iron–sulfur protein near the surface of cytochrome c_1, but not directly in a linear pathway between the iron–sulfur cluster and the c_1 heme. The pre-steady-state rates of reduction of cytochromes b and c_1 in mutants in which F177 and H184 were changed to non-aromatic residues were approximately 70–85% of the wild-type rates. There was a large decrease in iron–sulfur protein levels in mitochondrial membranes resulting from the W152L mutation and the W176L–F177L double mutation, and a small decrease for the Y205L, W176L and F177L mutations. This indicates that the decreases in activity resulting from these amino acid changes are due to instability of the altered proteins. These results show that these aromatic amino acids are unnecessary for electron transfer, but several are required for structural stability.

Keywords: Iron–sulfur protein; Cytochrome c_1; Cytochrome b; Aromatic amino acid; Site directed mutagenesis

1. Introduction

The cytochrome bc_1 complex is an oligomeric membrane enzyme that participates in energy transduction during respiration and photosynthesis in eukaryotic cells and numerous bacteria [1]. The cytochrome bc_1 complex transfers electrons from ubiquinol to cytochrome c, and links this electron transfer to translocation of protons across the inner mitochondrial membrane or bacterial plasma membrane through the protonmotive Q cycle [2,3]. Although the Q cycle mechanism describes the electron transfer pathway within the bc_1 complex, details of the electron transfer and protonmotive mechanisms within individual redox proteins are not fully understood.

The crystal structures of the cytochrome bc_1 complex show a dimeric integral membrane protein with cytochrome b primarily located within the mem-

* Corresponding author. Fax: +1-603-650-1389; E-mail: trumpower@sarthmouth.edu

0005-2728/99/$ – see front matter
PII: S0005-2728(99)00002-X

brane, and the iron–sulfur protein (ISP) and cytochrome c_1 within the intermembrane space [4,5]. Within the crystals from the native chicken enzyme redox active Fe2 of the iron–sulfur cluster is 21 Å distant from the iron of cytochrome c_1, while in the presence of stigmatellin the distance increases to 34 Å [5]. In contrast, the distance between Fe2 and heme b_L decreases from 34 to 26 Å in the presence of stigmatellin. The large distances between the iron–sulfur cluster and either cytochrome c_1 or b_L are inconsistent with rapid rates of electron transfer and suggest that movement of the ISP is required to bring the protein within closer proximity to the redox centers.

Long-range electron transfer between redox centers within proteins is predominantly controlled by distance, free energy and reorganization energy [6,7]. There is conflicting evidence whether there are specific electron transfer pathways within proteins. Some suggest that the protein has an essentially uniform dielectric composition and that the probability of electron transfer is predominantly controlled by distance [8]. Others have suggested that secondary structure plays a critical role in electron transfer within a protein [7]. In the latter context it is conceivable that π orbitals of aromatic amino acids may form conduits for electron transfer. He et al. [9] have shown that a surface-exposed tyrosine residue within plastocyanin was important for cytochrome *f* binding and electron transfer. In contrast, Farver et al. [10] have shown that mutation of a tryptophan residue within the putative electron transfer pathway had little effect upon electron transfer from a disulfide radical to Cu(II) in azurin.

Aromatic amino acids within the hydrophobic core of a protein predominantly contribute to structural stability, while aromatic amino acids at the surface are often critical for protein–protein interactions [11]. By sequence analysis, we have identified ten conserved aromatic amino acids in the ISP of the bc_1 complex, in addition to the two histidines that are ligands to the iron–sulfur cluster. Seven of the conserved aromatics are buried within the protein and three are at the protein surface [12]. In the experiments reported here we have tested whether conserved aromatic amino acids within the Rieske iron–sulfur protein form a conduit for electron transfer. Our results show that these aromatic residues are not necessary for electron transfer; however, several are necessary for structural stability.

2. Materials and methods

2.1. Materials

Sodium dodecyl sulfate (SDS), acrylamide and bisacrylamide were from Bio-Rad. Urea and agarose (Ultra pure) were from Life Technologies. DNA was isolated from agarose gels using the QIAquick gel extraction kit from Qiagen. Nytran nylon membranes were from Schleicher and Schuell. Glass beads (0.5 mm) were from Biospec Products. Horse heart cytochrome *c* and 2,3-dimethoxy-5-methyl-6-*n*-decyl-1,4-benzoquinone were from Sigma. Yeast extract, peptone, bacto-agar and tryptone were from Difco. Amino acids were from Bio 101.

2.2. Site-directed mutagenesis

The plasmid pGEM3–RIP1, carrying the wild-type *S. cerevisiae* ISP gene, was used for site-directed mutagenesis with the Clontech Transformer mutagenesis kit [13]. The mutations were confirmed by automated sequencing using the Dye Deoxy terminator cycle sequencing kit from Applied Biosystems. A *Pst*I/*Sac*I fragment from the mutated pGEM–RIP1 was subcloned into the single-copy yeast vector pFL39–RIP1, from which the *Pst*I/*Sac*I fragment was removed. Yeast cells from the RIP1 deletion strain JPJ1 were transformed with the pFL39–RIP1 plasmids containing the site-directed mutations [14].

2.3. Isolation of mitochondrial membranes

Yeast cells were grown at 30°C for 3 days on synthetic dextrose solid medium absent tryptophan. Mitochondrial membranes were isolated as previously described [15]. Mitochondrial membranes were resuspended in 10 mM MOPS (pH 7.2), containing 200 mM KCl, 0.02% Triton X-100 (w/v) and 30% glycerol (v/v), and stored at −20°C. Protein concentrations were determined by a modified Lowry method [16].

2.4. Western analysis and ubiquinol–cytochrome c oxidoreductase assays of mitochondrial membranes

Yeast mitochondrial membranes were resolved by SDS–polyacrylamide gel electrophoresis [17], and the ISP and cytochrome c_1 were detected by Western blotting [18] using monoclonal antibodies to the yeast ISP and cytochrome c_1 [15].

Ubiquinol–cytochrome *c* oxidoreductase activities of mitochondrial membranes were assayed at 22°C using 50 μM 2,3-dimethoxy-5-methyl-6-*n*-decyl-1,4-benzoquinol as substrate and 50 μM horse heart cytochrome *c*. The benzoquinone was reduced to quinol with borohydride as described previously [19]. The assays were performed in 50 mM potassium phosphate, 250 mM sucrose, 2 mM KCN, 0.2 mM EDTA, 1 mM NaN_3 and 0.1% (w/v) bovine serum albumin, at pH 7.0. Reduction of cytochrome *c* was monitored at 550 versus 539 nm in an Amino DW-2a spectrophotometer in dual beam mode. The spectrophotometer was controlled with an On-Line Instruments Systems computer interface. Assays were performed in triplicate, and activities of the cytochrome bc_1 complexes in isolated mitochondrial membranes are expressed as percentage versus the activities of membranes from JPJ1 transformed with plasmid carrying the wild-type RIP1 gene.

2.5. Purification of cytochrome bc_1 complex

Yeast cells were harvested by centrifugation at $2000\times g$ for 5 min from 100-l cultures grown in 0.7% yeast nitrogen base, 2% dextrose, and amino acids absent tryptophan (WT, F177L) or uracil (H184R). Yeast cells were washed once with distilled water and once with disruption buffer (100 mM Tris, 250 mM sorbitol, 5 mM $MgCl_2$, 150 mM potassium acetate, 1 mM DTT, pH 8.0). The washed yeast cells were resuspended by adding 80 ml of disruption buffer and frozen by slowing pouring the suspension as a thin stream into liquid nitrogen. The frozen yeast was blended in liquid nitrogen in a stainless-steel Waring blender for a total of 5 min at 1-min intervals. Additional liquid nitrogen was periodically added to prevent thawing of the cells.

The blended cell powder was thawed under warm water with the addition of 1 mM PMSF. The cell debris was sedimented at $3000\times g$ for 10 min, and the pellet was washed once in disruption buffer and sedimented at $3000\times g$ for 10 min. The supernatants were combined and the mitochondrial membranes were sedimented at $20\,000\times g$ for 30 min. The mitochondrial membranes were washed twice in 50 mM Tris acetate, 0.4 M mannitol, 2 mM EDTA (pH 8.0) containing 1 mM PMSF, and once in 150 mM potassium acetate, 50 mM Tris acetate, 2 mM EDTA, pH 8.0. Mitochondrial membranes were stored in 150 mM potassium acetate, 50 mM Tris acetate, 2 mM EDTA, 50% glycerol (pH 8.0), at −20°C.

To purify the bc_1 complex, mitochondrial membranes were suspended at 10 mg/ml in 50 mM Tris–HCl, 1 mM $MgSO_4$, 1 mM PMSF (pH 8.0) and 0.8 g of dodecyl maltoside/g of membrane protein was added and slowly stirred for 45 min at 4°C. The membrane extract was clarified by centrifugation at $100\,000\times g$ for 90 min. After the addition of 100 mM NaCl and stirring for 60 min, the extract was loaded onto a 1.5×20 cm DEAE–Biogel A chromatography column equilibrated with 50 mM Tris–HCl, 1 mM $MgSO_4$, 1 mM PMSF, 100 mM NaCl, pH 8.0. After loading, the column was washed with two column volumes of the same buffer and eluted with six column volumes of a linear gradient of 100–400 mM NaCl in 50 mM Tris–HCl, 1 mM $MgSO_4$, 1 mM PMSF, pH 8.0. The bc_1 complex eluted at approximately 280 mM NaCl. The combined bc_1 fractions were concentrated to 50 μM cytochrome *b* [20] using Amicon Centriprep 30 tubes.

2.6. Preparation of menaquinol

A 100-mM stock solution of menaquinone was prepared in ethanol. From this stock a 2-mM solution of menaquinone was prepared by dilution into 50 mM potassium phosphate (pH 6.0) containing 250 mM sucrose, 0.2 mM EDTA, 1 mM NaH_3 and 0.1% (w/v) bovine serum albumin. Since menaquinone is insoluble in aqueous buffers it precipitated from the solution. The menaquinone was reduced with a two-fold molar excess of sodium borohydride. As the menaquinone was reduced it became soluble in the aqueous buffer and was mixed until it was completely solubilized and no more bubbles were released. A fresh menaquinol solution was prepared prior to each kinetic experiment, kept under anaerobic con-

ditions, and diluted into degassed buffer immediately prior to its use. Control experiments established that the reduction of the cytochrome bc_1 complex is caused by menaquinol and not by any residual sodium borohydride.

2.7. Kinetic measurements

Kinetic measurements were performed at room temperature by stopped-flow rapid-scanning spectroscopy, using an Olis Rapid-Scanning Monochromator (On-Line Instrument Systems, Bogart, GA) equipped with a 1200 lines/mm grating blazed at 500 nm. This produced a spectrum of 75 nm width, centered at 555 nm, with a resolution of 0.4 nm. The dead time of the instrument was $\sim$2 ms, and the end of this period was chosen as time zero. Data was collected at 1000 scans/s.

Reactions were started by mixing 2 μM bc_1 complex in 50 mM potassium phosphate (pH 6.0) containing 250 mM sucrose, 0.2 mM EDTA, 1 mM NaN_3 and 0.1% (w/v) bovine serum albumin against an equal volume of buffer containing menaquinol. An oxidized spectrum was obtained by mixing the oxidized bc_1 complex against buffer and averaging the data set to a single scan. For each experiment four data sets were averaged, and the oxidized spectrum was subtracted from each scan. From the three-dimensional data set, which is comprised of wavelength, absorbance and time, we examined the time course of cytochrome b and c_1 reduction at 564.1 and 554.6 nm, respectively.

2.8. Sequence alignments, crystal structure calculations and graphics

Alignments of the amino acid sequences of the Rieske iron–sulfur proteins from various species were performed as described [21]. Views of the ISP and cytochrome c_1 were generated from the crystal structure coordinates of the chicken cytochrome bc_1 complex [5], using the molecular graphics program Rasmol, version 2.6 (Roger Sayle). Interatomic distances were measured using the program Rasmol. Distances between the conserved aromatic amino acids and Fe2 were measured using the bovine crystal structure [12]. The distances between the aromatic amino acids and residues on cytochrome b or c_1 were calculated using the crystal structure coordinates of the chicken cytochrome bc_1 complex [5], which were generously provided by Dr. Edward Berry (University of California, Berkeley, CA).

3. Results and discussion

3.1. Identification of conserved aromatic amino acids

Sequence analysis of the ISP from mitochondrial and bacterial cytochrome bc_1 complexes identified ten conserved aromatic amino acids, in addition to the two histidine residues that are ligands to the iron–sulfur cluster [12]. The conserved aromatics include W111, F117, W152, F173, W176, F177, H184, Y185, Y205 and F207 in the yeast protein[1] (Fig. 1). Of these ten amino acids only W176 and Y185 are conserved within cytochrome bc_1 and *bf* complexes, with a tyrosine residue equivalent to that at position 185 in the yeast protein found in every species examined. We have previously shown that the hydroxyl group of Y185 significantly increases the midpoint potential of the iron–sulfur cluster, presumably by electron delocalization through a hydrogen bond to a cysteine sulfur that is one of the ligands to the iron–sulfur cluster [22]. In addition, substitutions of other residues for Y185 indicate that the bulk provided by an aromatic side chain at this position is essential for stability of the yeast protein. Eight of the conserved aromatic amino acids are identical between bovine and yeast, while in yeast W176 and F177 are tyrosine residues. Of the ten aromatic residues, only F173, F177 and H184 are at the protein surface [12].

Four of the conserved aromatic amino acids are >20 Å from the iron–sulfur cluster, and thus are unlikely to be involved in electron transfer, but may contribute to structural stability (Fig. 2). W111 is 20 Å from Fe2 and is located on strand β2 between sheets 1 and 2. W152 is 26 Å from Fe2, and is located on strand β4 between sheets 1 and 2. Both Y205 and F207 are on strand β9 and are

[1] Hereafter, unless explicitly stated otherwise, we will use the numbering system from yeast for the ISP, and from chicken for cytochromes b and c_1.

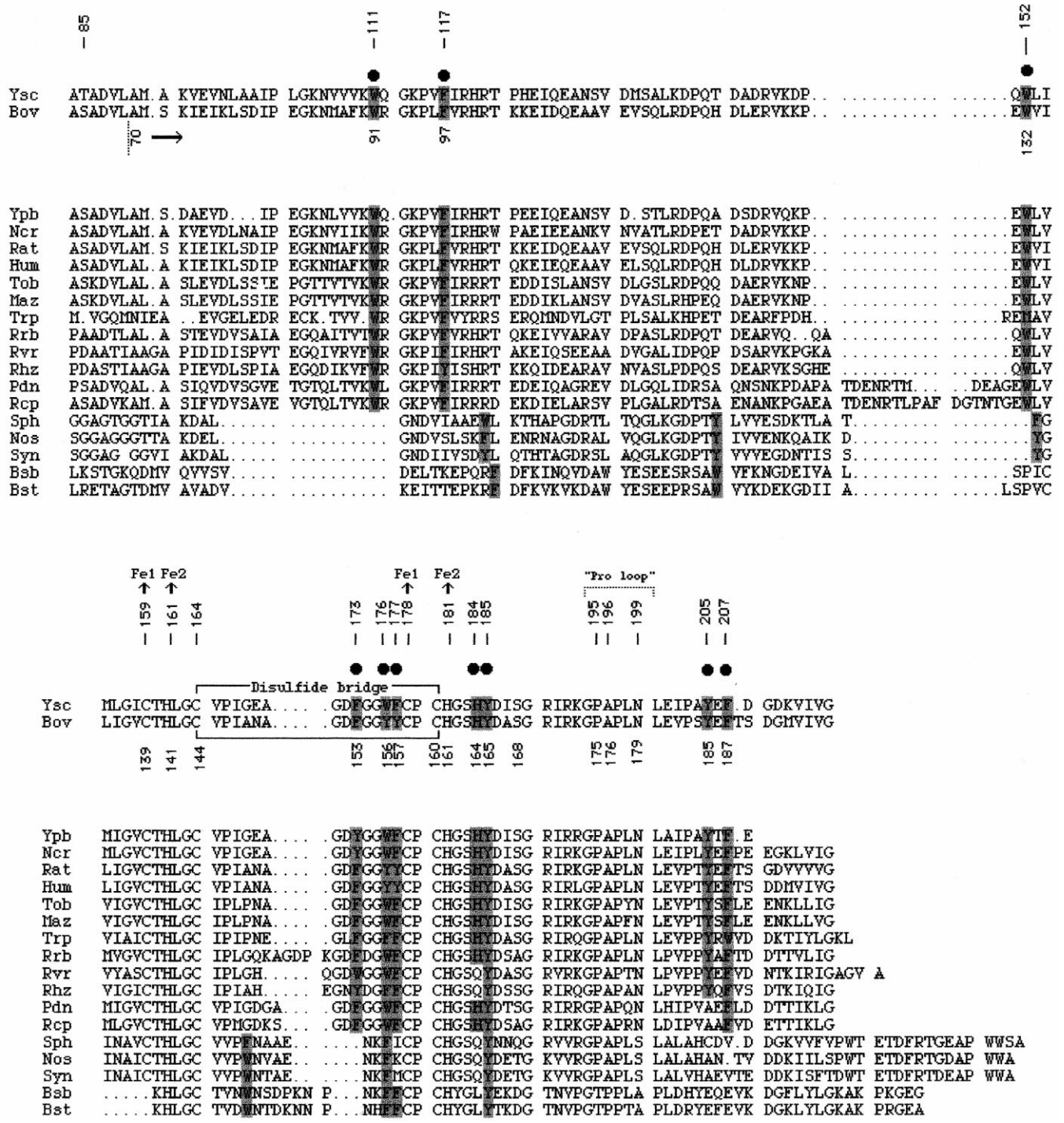

Fig. 1. Sequence alignment of the *Saccharomyces cerevisiae* Rieske iron–sulfur protein with that of other species. The abbreviations used include Ysc (*S. cerevisiae*), Bov (bovine heart), Ypb (*Schizosaccharomyces pombe*), Ncr (*Neurospora crassa*), Rat (rat), Hum (Human), Tob (tobacco mitochondria), Maz (maize mitochondria), Trp (*Trypanosoma brucei*), Rrb (*Rhodospirillum rubrum*), Rvr (*Rhodopseudomonas viridis*), Rhz (*Bradyrhizobium japonicum*), Pdn (*Paracoccus denitrificans*), Rcp (*Rhodobacter capsulatus*), Sph (spinach chloroplast), Nos (*Nostoc*), Syn (*Synechococcus*), Bsb (*Bacillus subtilis*) and Bst (*B. stereothermophilus*).

24 and 28 Å from Fe2, respectively, and lie between sheets 1 and 2. These four conserved aromatic amino acids are solvent inaccessible.

The remaining aromatic amino acids are closer to the iron–sulfur cluster, and thus may be involved in electron transfer to cytochrome c_1. F117 is 14 Å from Fe2 and is located on strand β3. The side chain of F117 is buried within the protein and is shielded from the protein surface by N106 in the bovine protein. F173 is 15 Å from Fe2, in the loop between strand β5 and β6, at the surface of the protein. In the bovine protein D172, K193 and R192 surround the hydrophobic side chain of this phenylalanine on the surface of the protein (Fig. 2). The side chain of F173 is >12 Å from either cytochrome *b* or c_1 in the structures of both the native and stigmatellin-bound enzyme [5] and distal from the heme of c_1 in relation to the iron–sulfur cluster (Fig. 2).

W176 of the yeast protein replaces Y156 of the bovine protein, which is located on strand β6 with the hydroxyl group 15 Å from Fe2. F177 of the yeast protein replaces Y157 of the bovine protein, and is

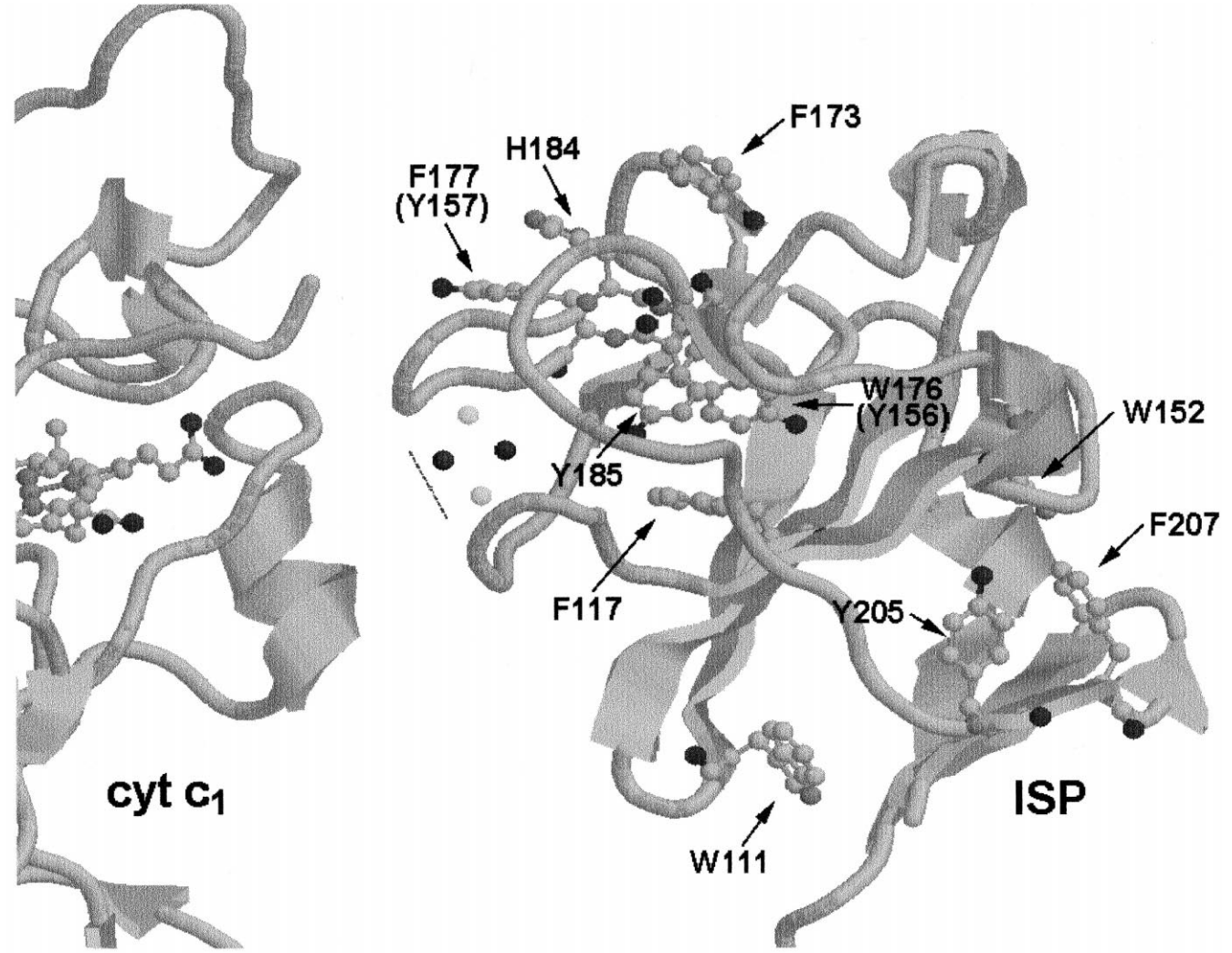

Fig. 2. View of the Rieske iron–sulfur protein and cytochrome c_1. The view shows the location of the conserved aromatic amino acids in the ISP and the [2Fe–2S] cluster in relationship to the heme of cytochrome c_1. The disulfide bridge that stabilizes the cluster-binding-fold is shown as a dashed line. Iron and sulfur atoms of the cluster are in black and gray, respectively, with redox active Fe2 located proximal to the disulfide bridge. The conserved aromatic amino acids shown include W111, F117, W152, F173, Y176, Y177, H184, Y185, Y205 and F207.

located on strand β6 and only 9 Å from Fe2. The side chain of the bovine Y156 is buried within the protein and pointed in the opposite direction of the side chain of the bovine Y157. We assume that W176 and F177 have the same relative orientation in the yeast protein (Fig. 2). The side chain of F177 lies at the protein surface, and in the bovine protein the homologous tyrosine residue is surrounded by A170, P179, G182 and H184. In the crystal structure of the native bc_1 complex, the side chain of F177 is 8 Å from G144 and L147 of cytochrome c_1 [5]. It is unlikely that F177 is involved in electron transfer from the ISP to cytochrome c_1, since it is not in the direct pathway between the two redox centers (Fig. 2). In the crystal structure of the stigmatellin bound enzyme, the residue homologous to F177 (Y157) is only 4 Å from V344 and 6 Å from P343 of cytochrome *b*, making it likely that this residue may contribute to binding between the ISP and cytochrome *b*.

H184 is conserved across the mitochondrial bc_1 complexes; however, in several of the bacterial bc_1 complexes and in the cytochrome *bf* complexes it is replaced by a glutamine residue (Fig. 1). H184 is located on strand β7 and is 10 Å from Fe2 with the side chain extending perpendicular from the protein surface. The side chain of H184 is adjacent and perpendicular to F177, and is surrounded by G171, D172 and K193 in the bovine protein. In the native enzyme crystal structure its closest distance is 11 Å from G144 of cytochrome c_1. In the crystal structure of the stigmatellin bound enzyme, H184 of the ISP is only 5 Å from V344 and 7 Å from E345 of cytochrome *b*, which suggests that this residue also may be involved in binding between the ISP and cytochrome *b*.

Since H184 is not fully conserved across mitochondrial bc_1 complexes, it is not expected to be essential for catalytic activity. In a previous study, when H184 was mutated to arginine, the iron–sulfur cluster was properly assembled, and the yeast grew on nonfermentable carbon sources, indicating that the protein was functional [15]. However, it was not determined if the mutation may have marginally affected ISP activity.

In our mutagenesis we preserved the hydrophobic character of the aromatic amino acids by substituting leucine residues. These mutations include W111L, F117L, W152L, F173L, W176L, F177L, Y205L and Y207L, and the double mutation W176L–F177L. This was done to minimize any structural damage to the protein by removing the large hydrophobic side chain.

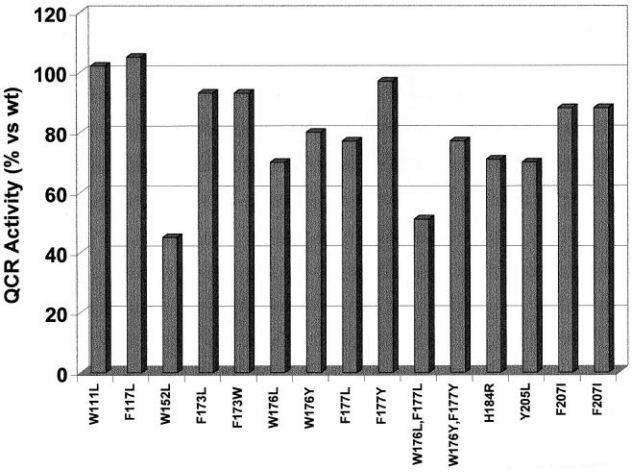

Fig. 3. Ubiquinol–cytochrome *c* oxidoreductase activities of mitochondrial membranes from yeast expressing mutated forms of the iron–sulfur protein. Activity is expressed as a percentage of that in membranes from yeast containing the wild-type ISP. The ISP mutations are identified by the number of the amino acid residue and the amino acid change made at that position.

Table 1
Growth phenotypes of yeast strains containing altered forms of the Rieske ISP

SP mutation	Phenotype
W111L	**Pet**$^+$
F117L	**Pet**$^+$
W152L	**Pet**$^+$ (ts 30°C, 37°C)
F173W	**Pet**$^+$
F173L	**Pet**$^+$ (ts 37°C)
W176L	**Pet**$^+$ (ts 37°C)
W176Y	**Pet**$^+$
F177L	**Pet**$^+$
F177Y	**Pet**$^+$
W176L, F177L	**Pet**$^+$ (ts 37°C)
W176Y, F177Y	**Pet**$^+$
H184R	**Pet**$^+$
Y205L	**Pet**$^+$ (ts 37°C)
Y207I	**Pet**$^+$
Y207L	**Pet**$^+$

JPJ1 was transformed with pFL39 plasmids containing the RIP1 gene with the site-directed mutations indicated in the left column. **Pet**$^+$ indicates growth on ethanol/glycerol medium. Within the parentheses, ts indicates the inability of the mutant to grow on ethanol/glycerol at the specified temperature.

The turnover number of the bovine cytochrome bc_1 complex is approximately five times greater than that of the yeast enzyme [20]. Since several of the conserved aromatic amino acids are different between the bovine and yeast proteins, we wanted to determine if these different aromatic residues contribute to the differences in catalytic activity. Thus, we substituted the yeast amino acids with the corresponding bovine amino acids to obtain yeast iron–sulfur protein with W176Y, F177Y and W176Y–F177Y replacements.

3.2. Growth characteristics and ubiquinol–cytochrome c oxidoreductase activities

To test the effects of the aromatic amino acid replacements, yeast mutants carrying altered iron–sulfur proteins were grown on solid medium containing ethanol/glycerol at 25°C, 30°C and 37°C (Table 1). All of the mutants were able to grow at 25°C, while the mutant with the W152L iron–sulfur protein mutation was unable to grow at 30°C and 37°C, and the mutants with the F173L, W176L, W176L–F177L and Y205L mutations were unable to grow at 37°C. The temperature sensitive phenotypes suggest that these mutations destabilize the protein, and this

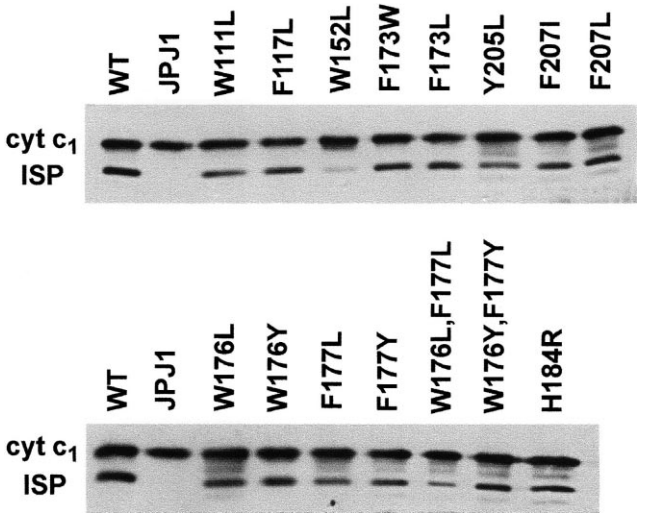

Fig. 4. Western blot of mitochondrial membranes from yeast expressing wild-type and mutated forms of the iron–sulfur protein. JPJ1 identifies membranes isolated from the yeast strain JPJ1 that was not transformed with plasmid. WT is JPJ1 transformed with pFL39–RIP1. The abbreviations for the ISP mutations are the same as in Fig. 3.

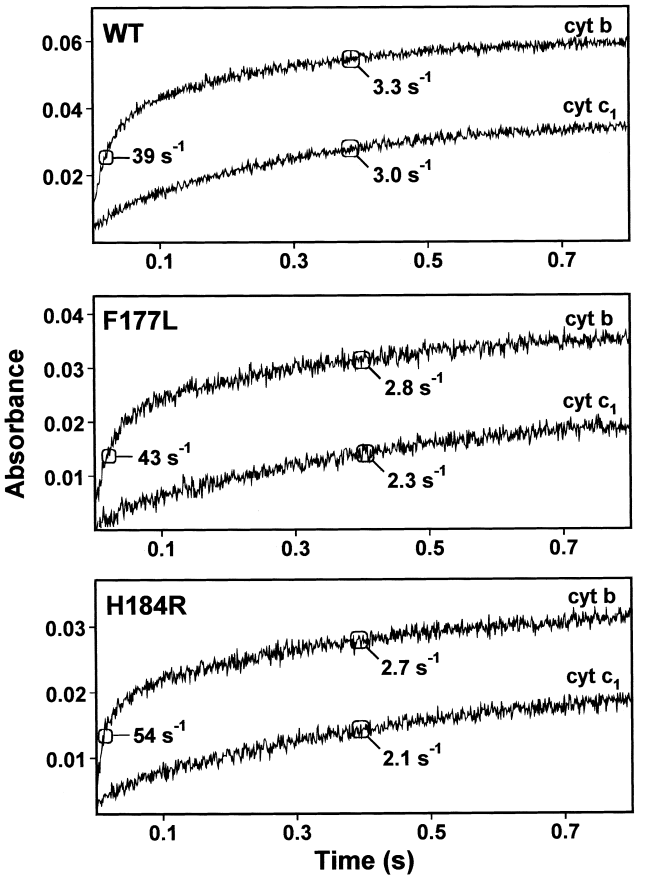

Fig. 5. Kinetics of reduction of the cytochrome bc_1 complex through center P in complexes containing wild-type iron–sulfur protein (top), or the F177L (middle) and H184R (bottom) iron–sulfur protein mutations. The three panels show the time course of reduction of cytochrome b and c_1 when 1 μM cytochrome bc_1 complex plus 3 μM antimycin is reduced by 50 μM menaquinol.

is confirmed by the Western blots shown below, which is consistent with these amino acids being buried within the protein, with the exception of F173. Since F173 is located at the protein surface, the F173L mutation may disrupt ISP binding to another subunit within the enzyme complex.

We have previously shown that ubiquinol–cytochrome c oxidoreductase activity of at least 30% is required to support growth of yeast on non-fermentable carbon sources [21]. Ubiquinol–cytochrome c oxidoreductase activities of mitochondrial membranes for all of the aromatic amino acid replacement mutants are greater than 40% of the wild-type activity (Fig. 3). Substitution of W111, F117, F173, Y205 or F207 with leucine maintained at least

80% of the catalytic activity. The mutations at W176, F177 and H184 decreased the activity to 60–80%. Since F177 and H184 are close to cytochrome *b* in the stigmatellin-bound enzyme, the decrease in catalytic activity to 70% resulting from the F177L and H184R mutations may be caused by an alteration of ISP binding to cytochrome *b*.

The mutations that decreased the activity by the largest amount were W152L and W176L–F177L. Since these mutations produced a temperature-sensitive petite phenotype, the decrease in catalytic activity is primarily due to ISP instability and not due to a direct affect upon the electron transfer.

Substitution of W176 and F177 with tyrosine residues, individually or in combination, did not increase the catalytic activity of the cytochrome bc_1 complex (Fig. 3). Thus, the increased turnover number of the bovine bc_1 complex compared to that of yeast is not solely attributable to differences in these aromatic amino acids.

3.3. Western blot analysis of mitochondrial membranes from yeast strains with aromatic amino acid replacements in the iron–sulfur protein

The content of iron–sulfur protein in mitochondrial membranes from JPJ1 expressing the mutated genes from pFL39–RIP was assayed by Western blotting. Cytochrome c_1 was used as an internal control to establish that equal amounts of mitochondrial protein were loaded onto the gel. Membranes isolated from JPJ1 showed no immunologically detectable ISP (Fig. 4). Membranes from yeast expressing W111L, F117L, F173W, F173L, F207I, F207L, W176Y, F177Y, W176Y–F177Y and H184R forms of the ISP contained similar amounts of ISP as yeast transformed with pFL39–RIP1 expressing the wild-type protein, indicating that these mutations had little effect upon the stability of the protein. In the membranes from the mutants carrying the Y205L, W176L and F177L forms of the protein there was a small decrease in ISP levels, consistent with the instability of the protein as suggested by the temperature sensitive phenotypes of the Y205L and W176L mutations.

In membranes from two of the mutants, carrying the W152L and the W176L–F177L double mutation, there was clearly a large decrease in iron–sulfur protein levels. These results are consistent with the temperature-sensitive phenotype of these mutants and show that the decrease in catalytic activity is caused by protein instability. In summary, all of the iron–sulfur proteins with aromatic amino acid substitutions retained significant amounts of catalytic activity, and the decreases in activity that were observed correlated with loss of iron–sulfur protein due to instability.

3.4. Pre-steady-state reduction kinetics of the cytochrome bc_1 complexes containing the F177L and H184R iron–sulfur protein mutations

Since F177 and H184 of the ISP are within proximity to cytochrome c_1 and thus may be involved in electron transfer and/or subunit interaction, we examined the pre-steady-state reduction kinetics of cytochromes *b* and c_1 in the bc_1 complexes isolated from the yeast strains with the F177L and H184R iron–sulfur protein mutations. Since the rate-limiting step in the catalytic cycle is the oxidation of ubiquinol [22], it is not possible to directly measure the rate of electron from the iron–sulfur protein to cytochrome c_1 in pre-steady-state reduction experiments. However, it is possible to determine if these ISP mutations affect the rate of quinol oxidation at center P and the subsequent reduction of cytochrome *b* and

Table 2
Second-order rate constants for the reduction of cytochromes *b* and c_1 by menaquinol

Iron–sulfur protein	Cytochrome *b*-fast ($\times 10^5$ $M^{-1}\,s^{-1}$)	Cytochrome *b*-slow ($\times 10^5$ $M^{-1}\,s^{-1}$)	Cytochrome c_1 ($\times 10^5$ $M^{-1}\,s^{-1}$)
Wild-type	5.7 ± 0.6	0.56 ± 0.04	0.45 ± 0.03
F177L	5.6 ± 0.4	0.45 ± 0.02	0.38 ± 0.02
H184R	7.4 ± 0.3	0.42 ± 0.03	0.30 ± 0.03

JPJ1 was transformed with pFL39 plasmids containing the RIP1 gene encoding the wild-type or mutated iron–sulfur proteins indicated in the left column. The second-order rate constants were calculated from a linear fit of the rates of cytochromes *b* and c_1 reduction with menaquinol concentrations of 25, 50, 75 and 100 μM.

c_1. For these experiments, we isolated cytochrome bc_1 complex containing the iron–sulfur protein mutations F177L and H184R. At pH 6.0, the catalytic activities of these complexes were $70 \pm 5\%$ and $59 \pm 10\%$, respectively, of the activity of the bc_1 complex from the wild-type strain (data not shown). Western blot analysis showed no obvious decrease in iron–sulfur protein levels in these mutants (Fig. 4), which suggests that the decrease in catalytic activity is not caused by ISP instability. In order to block the oxidation/reduction of cytochrome *b* at center N and isolate center P, we included antimycin in the pre-steady-state kinetics experiments.

With the bc_1 complex isolated from the wild-type yeast and the bc_1 complexes with the F177L and H184R iron–sulfur protein mutations the reduction of cytochrome *b* occurred as a biphasic reaction, with each phase comprising $\sim 50\%$ of the total absorbance change, while cytochrome c_1 reduction was monophasic (Fig. 5). Experiments were performed using different menaquinol concentrations, which allowed the calculation of second-order rate constants; the results of which are summarized in Table 2. In each case, there were linear relationships between menaquinol concentrations and the two phases of *b* reduction and the one phase of c_1 reduction. Due to the error in accurately measuring the fast phase of cytochrome *b* reduction it is not possible to determine if there are small differences between the rates of the fast phase of cytochrome *b* reduction in the wild-type complex and the complexes containing the F177L and H184R iron–sulfur protein mutations. However, the slow phase of cytochrome *b* reduction in the bc_1 complexes with the F177L and H184R iron–sulfur protein mutations was 80% and 75% of the wild-type rate, respectively, and the rate of cytochrome c_1 reduction was 84% and 67% of the wild-type rate for these mutants as well. These decreases in pre-steady-state reduction rates are comparable to the decreases in catalytic activity observed in mitochondrial membranes from these mutants.

Since the conserved aromatic amino acids are not essential for catalytic activity, we conclude that they do not form a conduit that is essential for electron transfer from the iron–sulfur cluster to the heme of cytochrome c_1. However, some of these aromatic residues contribute to the stability of the iron–sulfur protein. From the crystal structures of the bc_1 complex [5] it appears that movement of the iron–sulfur protein could allow direct electron transfer from the iron–sulfur cluster to the heme of cytochrome c_1. Since F177 and H184 of the iron–sulfur protein are within close proximity to cytochrome c_1, they may be involved in subunit interaction during iron–sulfur protein movement.

Acknowledgements

This research was supported by NIH Grant GM 20379 and by a NRSA fellowship to Chris Snyder.

References

[1] B.L. Trumpower, R.B. Gennis, Annu. Rev. Biochem. 63 (1994) 675–716.
[2] P. Mitchell, J. Theor. Biol. 62 (1976) 327–367.
[3] U. Brandt, B. Trumpower, Crit. Rev. Biochem. Mol. Biol. 29 (1994) 165–197.
[4] D. Xia, C.A. Yu, H. Kim, J.Z. Xia, A.M. Kachurin, L. Zhang, L. Yu, J. Deisenhofer, Science 277 (1997) 60–66.
[5] Z. Zhang, L. Huang, V.M. Shulmeister, Y.I. Chi, K.K. Kim, L.W. Hung, A.R. Crofts, E.A. Berry, S.H. Kim, Nature 392 (1998) 677–684.
[6] C.C. Moser, C.C. Page, R. Farid, P.L. Dutton, J. Bioenerg. Biomembr. 27 (1995) 263–274.
[7] H.B. Gray, J.R. Winkler, Annu. Rev. Biochem. 65 (1996) 537–561.
[8] C.C. Moser, J.M. Keske, K. Warncke, R.S. Farid, P.L. Dutton, Nature 355 (1992) 796–802.
[9] S. He, S. Modi, D.S. Bendall, J.C. Gray, EMBO J. 10 (1991) 4011–4016.
[10] O. Farver, L.K. Skov, T. Pascher, B.G. Karlsson, M. Nordling, L.G. Lundberg, T. Vanngard, I. Pecht, Biochemistry 32 (1993) 7317–7322.
[11] T.E. Creighton, Proteins: Structures and Molecular Properties, W.H. Freeman, New York, 1993.
[12] S. Iwata, M. Saynovits, T.A. Link, H. Michel, Structure 4 (1996) 567–579.
[13] J.H. Nett, E. Denke, B.L. Trumpower, J. Biol. Chem. 272 (1997) 2212–2217.
[14] H. Ito, Y. Fukuda, K. Murata, A. Kimura, J. Bacteriol. 153 (1983) 163–168.
[15] L.A. Graham, B.L. Trumpower, J. Biol. Chem. 266 (1991) 22485–22492.
[16] M.A. Markwell, S.M. Haas, L.L. Bieber, N.E. Tolbert, Anal. Biochem. 87 (1978) 206–210.
[17] U.K. Laemmli, Nature 227 (1970) 680–685.

[18] H. Towbin, T. Staehelin, J. Gordon, Proc. Natl. Acad. Sci. U.S.A. 76 (1979) 4350–4354.
[19] B.L. Trumpower, C.A. Edwards, J. Biol. Chem. 254 (1979) 8697–8706.
[20] P.O. Ljungdahl, J.D. Pennoyer, D. Robertson, B.L. Trumpower, Biochim. Biophys. Acta 891 (1987) 227–242.
[21] L.A. Graham, U. Brandt, J.S. Sargent, B.L. Trumpower, J. Bioenerg. Biomembr. 25 (1992) 245–257.
[22] E. Denke, T. Merbitz-Zahradnik, O.M. Hatzfeld, C.H. Snyder, T.A. Link, B.L. Trumpower, J. Biol. Chem. 273 (1998) 9085–9093.